

Independent Segregation of the Two Arms of the *Escherichia coli ori* Region Requires neither RNA Synthesis nor MreB Dynamics^{∇§‡}

Xindan Wang[†] and David J. Sherratt^{*}

Department of Biochemistry, University of Oxford, South Parks Rd., Oxford OX1 3QU, United Kingdom

Received 22 July 2010/Accepted 20 September 2010

The mechanism of *Escherichia coli* chromosome segregation remains elusive. We present results on the simultaneous tracking of segregation of multiple loci in the *ori* region of the chromosome in cells growing under conditions in which a single round of replication is initiated and completed in the same generation. Loci segregated as expected for progressive replication-segregation from *oriC*, with markers placed symmetrically on either side of *oriC* segregating to opposite cell halves at the same time, showing that sister locus cohesion in the origin region is local rather than extensive. We were unable to observe any influence on segregation of the proposed centromeric site, *migS*, or indeed any other potential *cis*-acting element on either replication arm (replichore) in the AB1157 genetic background. Site-specific inhibition of replication close to *oriC* on one replichore did not prevent segregation of loci on the other replichore. Inhibition of RNA synthesis and inhibition of the dynamic polymerization of the actin homolog MreB did not affect *ori* and bulk chromosome segregation.

The chromosome of the extensively studied bacterium *Escherichia coli* undergoes simultaneous replication and segregation and has no apparent mitotic apparatus for chromosome segregation, a situation very different from that of eukaryotes, where replication and segregation occur in temporally separate periods of the cell cycle. An unsolved mystery of the bacterial cell cycle is how chromosome segregation takes place. Several mechanisms have been proposed to drive the segregation of origin and bulk DNA after replication. In one model, cell elongation is proposed to be a crucial factor, in which the two newly replicated origins are attached to the inner membrane and separated by cell growth between them along the long axis of the cell (25). However, it is now clear that elongation occurs throughout the cell and the movement of the origins is much faster than the rate of cell elongation, indicating that cell elongation alone is not responsible for segregation (55, 60).

Active partitioning systems were first found in low-copy-number plasmids, where they are required for stable inheritance by distributing the daughter plasmids to both daughter cells (reviewed in reference 14). These systems fall into two families; one uses the ParM actin and its associated protein and binding sites to drive newly replicated sister plasmids apart during cycles of actin polymerization and depolymerization (4, 19). The second *parABS* family is less well understood mechanistically, although ATP hydrolysis-dependent cycles of ParA

movement appear to play a key role in the segregation process (48).

Later, it was found that many bacterial chromosomes also utilize *parABS* systems for their segregation, for example, *Bacillus subtilis* (23, 37), *Caulobacter crescentus* (41), and both chromosomes of *Vibrio cholerae* (22). The typical chromosomal *par* locus consists of two genes, *parA* and *parB* (*soj* and *spo0J* in *B. subtilis*), and a *cis*-acting *parS* DNA element. ParB is a DNA-binding protein that specifically recognizes *parS* and subsequently spreads along the DNA to form a nucleoprotein complex (7, 37, 42). ParA is an ATPase that binds ParB and is proposed to direct the ParB/*parS* complex to the poles (18). These partitioning systems serve to facilitate chromosome segregation but are often not essential, for example, in *B. subtilis*, *Streptomyces coelicolor*, and *Pseudomonas putida* and for *V. cholerae* chromosome I (18, 23, 30, 35).

In contrast, these systems are essential for viability in *C. crescentus* (41, 54) and for segregation of chromosome II in *V. cholerae* (63). The latter requirement may be due to the fact that chromosome II has many properties of a large plasmid and its Par proteins are more closely related to plasmid-encoded ones than to those encoded on chromosomes (22). In *C. crescentus*, the *par* system may be essential only indirectly, as it is used for proper localization of the cell division machinery through at least two other proteins, PopZ (6, 13) and MipZ (53). PopZ captures the *parB/ori* complex and subsequently anchors it at opposite cell poles (6, 13). This results in the FtsZ polymerization inhibitor MipZ, which also forms a complex with ParB, to localize to the poles. High concentrations of MipZ at the poles and low concentrations at mid-cell restrict FtsZ ring formation to mid-cell for proper cell division (53).

In a similar indirect manner, Spo0J (ParB) in *B. subtilis* was recently demonstrated to recruit structural maintenance of chromosome (SMC) complexes to the *parS* sites in the origin region, where these complexes are proposed to organize the origin region and promote efficient chromosome segregation

* Corresponding author. Mailing address: Department of Biochemistry, University of Oxford, South Parks Rd., Oxford OX1 3QU, United Kingdom. Phone: 44-1865613237. Fax: 44-1865613238. E-mail: david.sherratt@bioch.ox.ac.uk.

[†] Present address: Department of Microbiology and Molecular Genetics, Harvard Medical School, 200 Longwood Ave., Boston, MA 02115.

[§] Supplemental material for this article may be found at <http://jba.asm.org/>.

[∇] Published ahead of print on 1 October 2010.

[‡] The authors have paid a fee to allow immediate free access to this article.

(21, 52). Furthermore, in sporulating *B. subtilis*, a different mechanism is used. RacA protein binds to a number of sites within ~200 kb of the origin and then attaches the chromosome to the cell pole in the forespore compartment in a process that also requires Soj and the polar localized cell division protein DivIVA (5, 62). This process prevents the formation of DNA-free forespores.

E. coli and some of its gammaproteobacterial relatives do not encode any obvious *parABS* system for chromosome segregation (39). It is interesting that these same bacteria have a divergent functional analog to SMC complexes made up of MukB, MukE, and MukF (50) and use SeqA to modulate the initiation of replication (reviewed in reference 56). An *E. coli* 25-bp *cis*-acting site (*migS*) capable of facilitating bipolar segregation of the origin region has also been described (16, 64). However, in the same studies, deletion of *migS* was shown to have little effect on overall segregation, suggesting that the sequence is not important or is functionally redundant.

A body of experimental evidence has indicated that the chromosome loci segregate sequentially after replication, with a relatively short period of cohesion (36, 43, 47, 57). These data, in part, provided support for an "extrusion-capture" model for chromosome segregation in which a DNA replication factory located at a fixed cellular position pulls in the DNA to replicate and then expels the newly replicated sisters outward (34). However, the demonstration that sister replisomes track independently along the DNA in slow-growing *E. coli* argues against this model (47). Other observations have led to the suggestion that the organization and properties of the *E. coli* chromosome lead to "segmented" chromosome segregation in which extensive regions of the chromosome segregate together (2, 15).

In a different model, both transcription itself and the coordinated transcription of membrane proteins and their insertion into the membrane ("transertion") have been proposed as processes that can drive chromosome segregation (12, 45, 49, 61). Nevertheless, these proposals have not been tested rigorously by experiments.

Additionally, it has also been proposed that the highly conserved actin-like cytoskeletal element MreB may play a key role in at least origin segregation (20, 31, 32, 51). MreB polymerizes to form spiral-like filaments that span the inner surface of the cytoplasmic membrane and is responsible for maintaining the cell shape (9, 17, 26). Recent studies have taken advantage of a small molecule, A22 (24), which rapidly disrupts MreB localization *in vivo* by directly binding to its ATPase pocket, inducing a state with low affinity for polymerization (3). Several studies have demonstrated that inhibition of MreB polymerization does not perturb initiation and progression of DNA synthesis but does apparently block segregation of newly replicated origins, but not bulk DNA (20, 31). Nevertheless, since MreB can serve as a cytoskeletal track for other proteins, its apparent role in origin segregation could be indirect, as supported by a reexamination of the role of MreB in *E. coli* DNA segregation (29).

Finally, thermodynamic considerations of the properties of a highly confined, self-avoiding polymer (representing a DNA molecule) in a rod-shaped cell-like geometry (representing a bacterial cell) have indicated that duplicated circular chromosomes could segregate spontaneously without any additional

force in physiologically relevant timescales (1, 27, 28). Therefore, entropy alone may be sufficient to produce the observed segregation of replicated chromosomes, while plasmids use active partition systems because their small size in a "sea" of chromosomal DNA would not lead to effective spontaneous segregation.

In this study, we combined snapshot and time-lapse fluorescence microscopy of cells in which a single round of replication is initiated and completed in the same generation to examine the segregation of newly replicated *ori* loci. We also examined the effects of blocking replication at a repressor-bound array at multiple loci, together with inhibitors of RNA synthesis and MreB activity, to add insight into the segregation process. We found no apparent direct role of transcription/transertion, *cis*-acting sequences, or MreB dynamics in *E. coli* chromosome segregation. We showed sequential and symmetric segregation of markers in the origin region and were able to spatially resolve loci that are physically separated by only a few kilobases.

MATERIALS AND METHODS

Bacterial strains and growth conditions. *E. coli* AB1157 strains containing *lacO* and *tetO* arrays were constructed as described previously (33, 57, 58). In brief, a *lacO* or *tetO* operator array on a plasmid (33) was PCR amplified using primers that provided 45 to 50 nucleotides (nt) of homology on each side of the target insertion locus. The PCR product was transformed to *E. coli* and integrated into the chromosome using λ red recombination (11). To construct the tandem *lacO-tetO* array, a *tetO* array (120 copies) was liberated from pLAU40 using NheI/HindIII and ligated to XbaI/HindIII-digested pLAU37, which contains 120 copies of *lacO*. The resulting plasmid was digested with XbaI/NdeI and ligated with the chloramphenicol resistance gene amplified from pKD3 using primers flanking the NheI/NdeI sites. A *tetO-lacO* tandem array, followed by a chloramphenicol resistance gene, was constructed using the same method by introducing the *lacO* array into the plasmid containing the *tetO* array. The tandem arrays were integrated into the chromosome using λ red recombination (11).

LacI-CFP and TetR-YFP (where CFP is cyan fluorescent protein and YFP is yellow fluorescent protein) were expressed constitutively from pWX6 (58). Unless otherwise stated, cells were growing at 37°C in M9 minimal medium supplemented with 0.2% glycerol and essential nutrients (58). For exponential growth, 0.5 mM isopropyl- β -D-thiogalactopyranoside (IPTG) and 40 ng/ml anhydrotetracycline (AT) were added to the medium to reduce repressor binding but allow normal replication and focus visualization. For replication blocks, exponentially growing cells were collected and washed using the same medium lacking AT by centrifugation (8,000 rpm, 1 min, three times) and subcultured in prewarmed AT-free medium. Cells were generally imaged 70 to 100 min after the block was applied, unless otherwise stated. The concentrations of the antibiotics used were 300 μ g/ml for rifampin, 10 μ g/ml for A22, and 100 μ g/ml for ampicillin.

Fluorescence microscopy. Cells were grown to an A_{600} of 0.1 to 0.2 and transferred onto a slide containing 1% agarose in the same medium. Cells were visualized with a 100 \times objective on a Nikon Eclipse TE2000-U microscope equipped with a Photometrics Cool-SNAP HQ charge-coupled device camera and a temperature-controlled incubation chamber. Images were analyzed and processed by Metamorph 6.2.

RESULTS

Segregation patterns of five loci in the *E. coli ori* region. Our previous studies have shown that genetic loci in the terminus region (*ter*), up to 400 kb apart, have a distinct spatial organization, with loci replicated by different forks frequently locating to opposite cell poles during most of the cell cycle (38, 58). This then raises the questions of whether origin regions on either side of *oriC* behave in the same way during chromosome segregation and whether any part of the origin region segre-

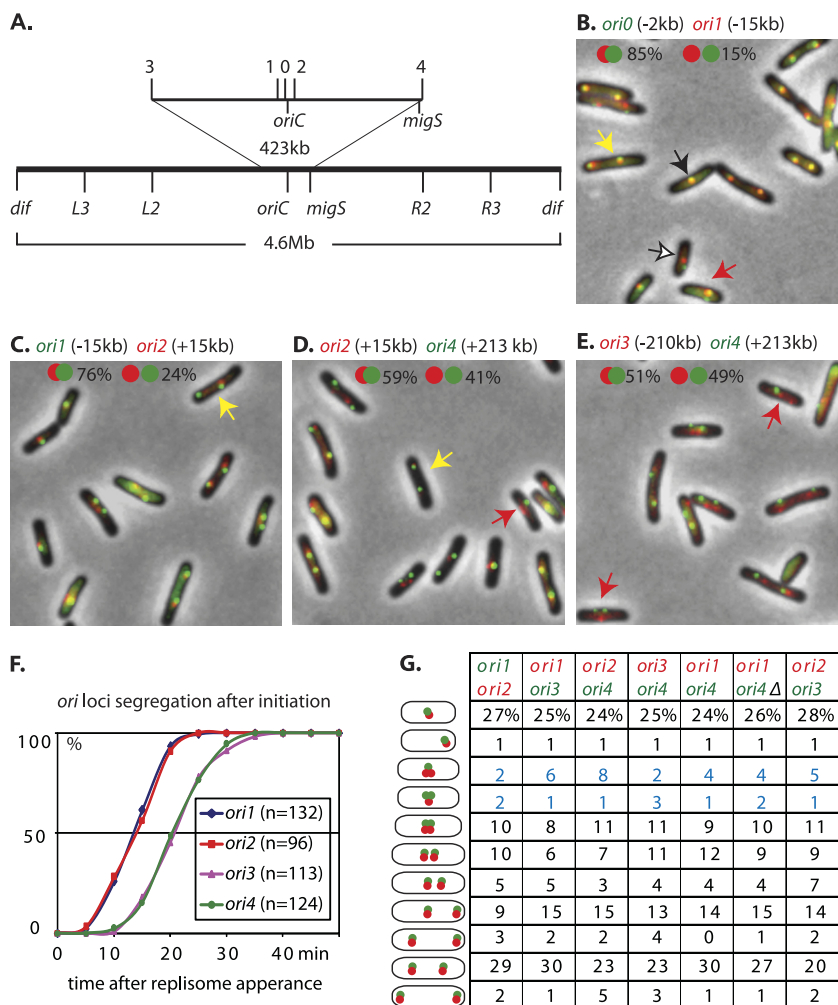


FIG. 1. Segregation pattern of five loci in the origin region in exponential cultures. (A) Schematic of the 4.6-Mbp *E. coli* chromosome indicating the positions of the markers used. *ori0*, *ori1*, *ori2*, and *ori3* are -2 kb, -15 kb, +15 kb, and -210 kb from *oriC*, respectively; *ori4* is +213 kb from *oriC* and +2 kb from *migS* (+, clockwise; -, counterclockwise). The positions of *L2*, *L3*, *R2*, and *R3* are at kb 2735, 2268, 366, and 852 on the genetic map of *E. coli* (57). (B to E) Snapshot examples of combinations of *ori0-ori1*, *ori1-ori2*, *ori2-ori4*, and *ori3-ori4*. Percentages of colocalization (foci at least partially overlapping, example indicated by the black arrow in panel B) and approximate colocalization (nonoverlapping but no more than one focus diameter apart, open arrow in panel B) are shown at the top of each picture. Red arrows show different timings in the initial separation of the two loci. Yellow arrows show asymmetric positioning of sister loci. Cells were grown exponentially at 37°C with a generation time of ~100 min. (F) Time-lapse analysis of *ori* locus segregation with respect to replisome appearance at initiation. Each *ori* locus was visualized together with the replisome marker YPet-DnaN. The time difference between replisome appearance and visible separation of the *ori* locus was recorded. The percentage of cells with separated foci was plotted for each time point. Images were captured every 5 min. (G) *ori* locus separation patterns of different strains. Highlighted in blue are the cell types in which the two loci have different timings of separation. At least 500 cells were analyzed for each culture. Δ stands for *ΔmigS*.

gates first. In order to address these questions, extensive analyses were carried out with markers in the 423-kb region in the origin region, including *oriC* and *migS*, the latter a 25-bp sequence 210 kb clockwise from *oriC*, which was reported to act like an *E. coli* centromere (Fig. 1A) (16, 64). Cells for all experiments were grown at 37°C in minimal-glycerol medium, which resulted in a generation time of ~100 min and with most DNA replication initiations occurring a few minutes after birth and terminating within the same generation (57, 58). Representative snapshot micrographs are shown in Fig. 1B to E, and the primary snapshot data are summarized in Fig. 1G. Time-lapse analyses are summarized in Fig. 1F.

Pairwise combinations of markers *ori0* (-2 kb from *oriC* [-

counterclockwise]), *ori1* (-15 kb from *oriC*), and *ori2* (+15 kb from *oriC* [+ , clockwise]) showed superimposition or partial overlapping of foci, suggesting that the position of any of the three markers broadly describes the behavior of *oriC*, although ~2% of the cells had the -2 kb sister loci (*ori0*) separated apparently earlier than sisters of the ±15 kb loci (*ori2* and *ori1*, Fig. 1B, red arrow, and G). Despite there being only 13 kb between the two closest *ori* loci, these loci are apparently resolvable both in time and in space.

Pairwise combinations of an *oriC*-proximal loci (*ori0*, *ori1*, and *ori2*) with *oriC*-distal loci *ori3* (-210 kb from *oriC*) and *ori4* (+213 kb from *oriC*) showed similar timing for initial separation, with 91 to 95% of the cells having the same number of

foci for each marker (Fig. 1G). In the 5 to 9% of the cells where there were two separated foci for one marker and only one focus for the other (Fig. 1G, rows highlighted in blue), the majority of the cells had the more *oriC*-proximal marker separated into two foci, consistent with sequential replication-segregation and the view that cells with a single focus rarely had two spatially nonresolvable foci. Furthermore, combination of *ori1* with *ori2* or of *ori3* with *ori4* showed that the timing for replication and separation of loci with the same distance from *oriC* but on opposite replichores were similar in most cells. Only 4% of *ori1-ori2* cells and 5% of *ori3-ori4* cells had two foci for one marker and one for the other.

The snapshots indicate that sister origins may not always segregate symmetrically from mid-cell to quarter positions (Fig. 1B to E, yellow arrows). For each *ori* marker, about 10 to 15% of the whole population showed asymmetric positioning of sisters, with one of the sisters close to mid-cell and the other close to a pole. In such cells, the two different *ori* markers exhibited the same asymmetric pattern (Fig. 1B to E, yellow arrows, and G), rather than the “opposed” asymmetry observed for loci in *ter* (58), despite there being up to ~400 kb separating the markers visualized in both *ori* and *ter*.

Time-lapse analysis was used to assess the interval between the initiation of replication and the segregation of the various *ori* markers. For this, cells carrying an *ori* marker and expressing a fluorescent replisome component, YPet-DnaN, were grown on microscopic slides. Images were taken every 5 min, and the appearance of the replisome was defined as time zero. The period of DNA synthesis in these cells was ~68 min (± 6 min, $n = 41$; i.e., ~ 34 kb \cdot min $^{-1}$), as judged by the time between replisome appearance and disappearance. The time difference between replisome appearance and visible separation of the *ori* marker was recorded. Fifty percent of the cells had two separated foci at 13 min for *ori1* and *ori2* and at 21 min for *ori3* and *ori4* (Fig. 1F). The separation of the *ori*-proximal loci at ~13 min after replication initiation is in agreement with previous estimates of cohesion in the *ori* region (47). Loci ~200 kb downstream of the *ori*-proximal loci (*ori3* and *ori4*), which were replicated ~6 min after the *ori*-proximal loci based on the ~ 34 -kb \cdot min $^{-1}$ replication rate in these cells, separated ~8 min later, indicating that these loci (*ori1*, -2, -3, and -4) have similar periods of cohesion. To test if deletion of the proposed centromeric sequence would affect the timing of locus separation, the *migS* locus was deleted from our AB1157 strain. Cells with or without *migS* behaved identically for *ori* separation in our analysis (Fig. 1G).

Our data support the view that segregation of loci in the origin region is sequential and symmetric with respect to each replichore, with loci closer to *oriC* segregating earlier. We found no evidence for asymmetrically positioned *cis*-acting sites during DNA segregation. Whatever the global domain structure of the *ori* region, it does not preclude the spatial separation and independent segregation of loci.

Espeli and colleagues (15) have reported rather different conclusions using *E. coli* MG1655. Although the focus of this study was the dynamic behavior of different genetic loci, using the ParB-*parS* labeling system, the authors inferred that *ori* region loci segregated together some substantive time (up to 30 min) after replication, with only subsequently replicated loci in apparent nonstructured regions showing shorter cohesion

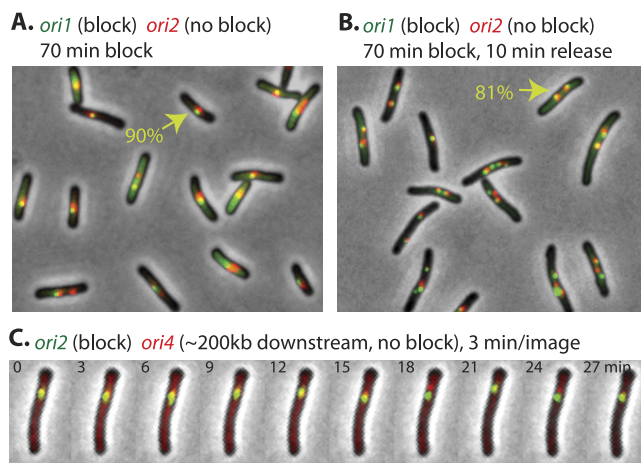


FIG. 2. Efficient site-specific replication block and release. (A) Replication blockage at *ori1* (*tetO*, green). Cells were grown exponentially with a generation time of ~100 min with AT and IPTG to reduce repressor binding for normal replication but allow focus visualization. AT was removed from cultures by washing to block replication at the *tetO* array (*ori1*, green) but not at the *lacO* array (*ori2*, red) for 70 min (see Materials and Methods for details). About 90% of the whole population had one focus for the block (green marker). (B) AT was added back to the culture for 10 min to release the block after 70 min of blocking. About 81% of the cells had the *ori1* (*tetO*, green) and *ori2* (*lacO*, red) loci segregated. (C) Time-lapse progression of *ori2* (*tetO*, green) *ori4* (*lacO*, red) mutant strain. A replication block was induced at *ori2* (*tetO*) in liquid culture for 70 min by removing AT, followed by another 100 min of growth on an agarose slide containing the same medium (without AT). An image was acquired every 3 min. *ori4* (*lacO*), which was ~200 kb downstream of the *ori2* (*tetO*) block, was never duplicated during the course of the experiment.

and sequential replication-segregation. We do not fully understand the reasons for these differences. However, Espeli and colleagues used a richer growth medium (minimal glucose, Casamino Acids) and a lower growth temperature (25°C). With a doubling time of ~120 min, these cells initiated and completed replication in different generations, with synchronous initiation at two origins occurring around 54 min after birth. These cells also had a very long period (~100 min) between the completion of replication and cell division (D period).

Site-specific replication fork blockage does not interfere with replication and segregation of loci on the opposite replichore. We have previously shown that tight binding of fluorescent fusions of either TetR or LacI to arrays of their cognate operators can be achieved when they are expressed in the absence of their inducers (AT and IPTG, respectively) and results in replication blockage at the array (46). Furthermore, replication restarts rapidly upon relief of these tight repressor-binding events. In order to examine the consequence of replication blockage on one side of *oriC* to segregation of other *ori* loci, we analyzed a variety of genetic loci after site-specific replication blockage.

In the first experiment, replication was blocked at *ori1* (*tetO*) using TetR-YFP (constitutively expressed from a high-copy-number plasmid, pWX6) by removing AT from the medium. Seventy minutes after the removal of AT, the proportion of cells with one *ori1* focus increased from ~25% to 90% (Fig. 2A, green marker). Importantly, loci downstream of the block,

but not close to the terminus region, never duplicated in the 2 to 4 h following the block. Equivalent results were observed with other blocks in *ori*. An example is shown in Fig. 2C, where a similar block was induced at *ori2* (*tetO*) by growing cells in liquid medium without AT for 100 min. These cells were then transferred to an agarose slide containing the same medium (without AT), and images were captured every 3 min. The locus ~200 kb downstream, *ori4* (*lacO*), never duplicated in the course of the experiment. These findings imply that tight TetR-YFP binding blocked replication and not segregation of the *ori2* (*tetO*) locus and that the marker downstream was not replicated during the course of the experiment by the clockwise fork (because of replication blockage at the upstream *tetO* array), by the counterclockwise fork (because of *ter* sites), or because of potential replication barriers created by sequence skew or head-on transcription collisions.

When AT was reintroduced to release the replication block, within 5 min, 66% of the cells had the *tetO* array segregated (data not shown), and after 10 min, this proportion increased to 81% of the cells (Fig. 2B, green marker). This is consistent with rapid replication restart and the immediate segregation of loci after replication. This contrasts with the general ~15-min cohesion period of newly replicated sister loci before their visible spatial segregation (see above; 47). The period of cohesion is modulated by the activity of topoisomerase IV (TopoIV), which removes the precatenanes that form between newly replicated DNAs (59). We propose that when replication is blocked by tightly bound repressors, there is sufficient time in the 70-min incubation period before release of the replication block for TopoIV to remove precatenanes so that, once replication resumes, segregation of newly replicated sister loci occurs immediately.

We next examined the consequence of blocking replication at *ori1* on the replication-segregation of loci on the other replicore (Fig. 3A). After being blocked at *ori1* (*tetO*; -15 kb from *oriC* on the left replicore) for 70 min, cells with one *ori1* (*tetO*) focus increased to ~90% as reported above. When the nonblocked locus being monitored was *ori4* (*lacO*; +210 kb from *oriC*, 240 kb from the block on the right replicore), after 70 min of *ori1* blockage, 33% of the cells had one *ori4* focus, 22% had two closely spaced *ori4* foci, and more than 30% of the cells had two clearly separated *ori4* foci. Similarly, after 70 min of replication blockage at *ori1*, replication-segregation of *R2* (*lacO*; +1,081 kb, midpoint of the whole 2.3-Mb right replicore) occurred identically to that in cells in which there was no replication block (Fig. 3E and G). These data confirm the independent action of replisomes on sister replicores (47) and show that loci on different replicores not only segregate independently but do so in such a way that each is not influenced by inhibition of the replication-segregation of the other replicore.

The segregation of *ori2* (*lacO*; +15 kb from *oriC* and 30 kb from *ori1*) in *ori1*-blocked cells was also examined (Fig. 3A). After replication blockage for 70 min, the percentage of cells with one *ori1* focus increased to 90% as reported above. At the *ori2* locus, >50% of the cells had one *ori2* focus and 16% of the cells had two *ori2* foci very close together. Only 12% of the cells had two well-segregated sister *ori2* foci, while 15% had an intermediate separation. Therefore, although blocking replication close to *oriC* on the left replicore does not prevent

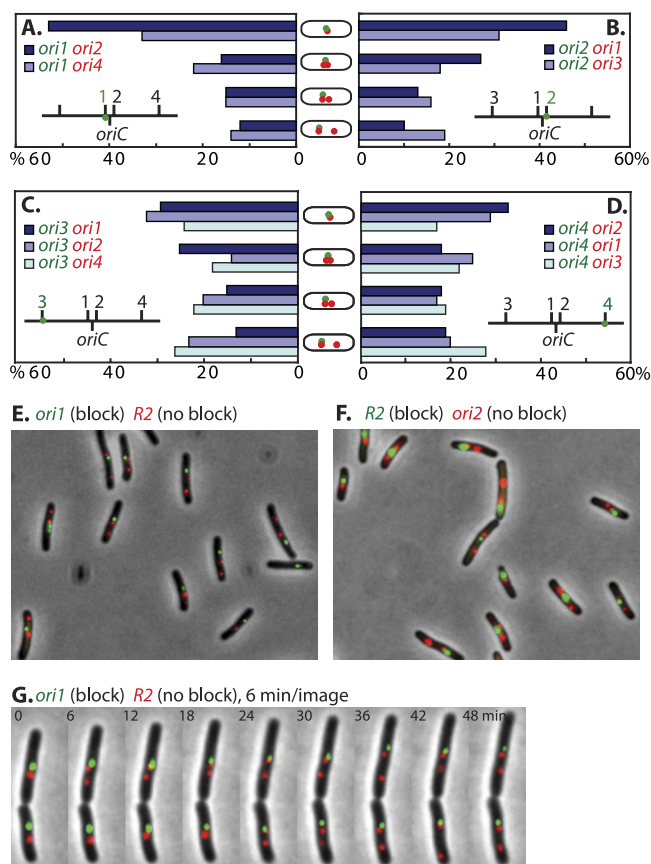


FIG. 3. Effect of the replication block on the segregation of other loci. (A to D) Segregation patterns of the other *ori* markers when replication was blocked at *ori1* (A), *ori2* (B), *ori3* (C), or *ori4* (D). More than 90% of the cells in each culture had only one block focus (green), and these cells were further divided into four classes according to the pattern of the nonblocked (red) locus as illustrated: one red focus, two red foci touching each other, two red foci segregated by less than 20% of the cell length, and two red foci segregated by more than 20% of the cell length. The proportion of each cell type is presented in the histogram. The genetic positions of *ori1*, -2, -3, and -4 relative to that of *oriC* are illustrated with the block labeled green. (A) Segregation pattern of *ori2* and *ori3* with blockage at *ori1*. (B) Segregation pattern of *ori2* and *ori1* with blockage at *ori2*. (C) Segregation pattern of *ori1*, *ori2*, and *ori4* with blockage at *ori3*. (D) Segregation pattern of *ori2*, *ori1*, and *ori3* with blockage at *ori4*. The block was induced for 70 min in liquid culture. Five hundred to 600 cells of each strain were analyzed. (E) Blockage at *ori* loci did not perturb the segregation of the later loci on the other replication arm. *R2* (*lacO*, red) segregated normally and achieved asymmetric localization as normal when *ori1* (*tetO*, green) was blocked for 70 min. (F) Blocking of later loci did not perturb the segregation of *ori* loci. *ori1* (*lacO*, red) segregated normally to quarter positions when *R2* (*tetO*, green) was blocked for 70 min. (G) Segregation of *R2* (*lacO*, red) when *ori1* (*tetO*, green) was blocked in a time-lapse progression. Replication was blocked at *ori1* for 60 min in liquid culture, followed by another 30 min on the slide, before the time-lapse progression. An image was taken every 3 min. Shown here is a 6-min time interval.

replication-segregation of loci on the right replicore, the proximity of *ori2* to the blocked *ori1* locus (30 kb away) does not perturb the visible spatial separation of newly replicated *ori2* sisters. This perturbation disappears when loci further along on the right replicore are examined. We assume that these differential effects on segregation are a direct consequence of

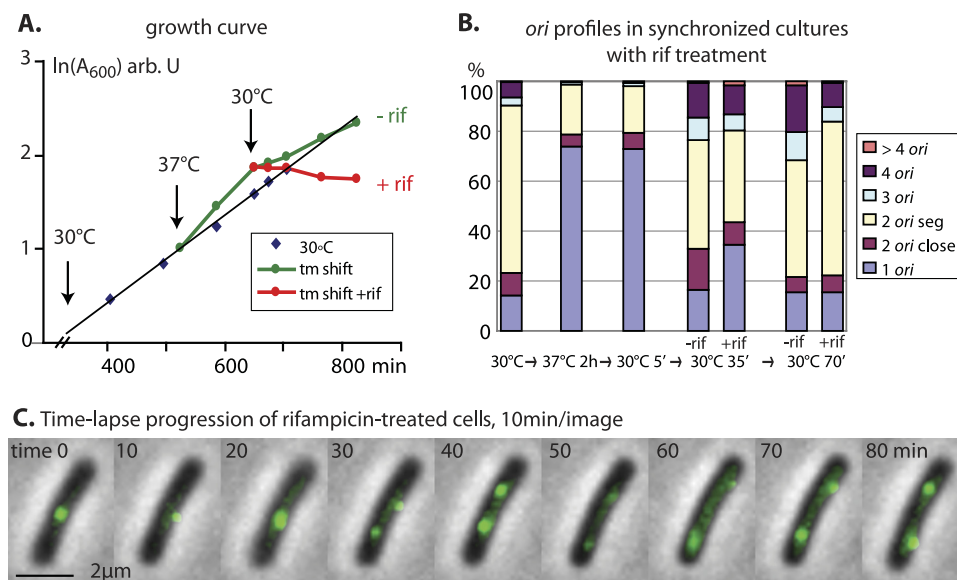


FIG. 4. Inhibition of transcription does not prevent origin segregation. (A) Growth curves of *dnaC(Ts)* mutant cells before and after rifampin (rif; 300 μ g/ml) treatment. Cells were grown exponentially at 30°C (blue diamonds). At an A_{600} of ~ 0.1 , part of the culture was shifted to 37°C for 2 h to allow synchronization of replication initiation (green dots). The culture temperature (tm) was then shifted back to 30°C to allow replication initiation, and rifampin was added to half of it (red dots). A_{600} was plotted on a logarithmic scale in arbitrary units (arb.U). (B) *ori* segregation pattern before and after rifampin treatment in a *dnaC(Ts)* mutant. Cells were grown exponentially at 30°C. The culture was shifted to 37°C for 2 h for synchronization and then to 30°C for 5 min for initiation of replication. The culture was split in two, and rifampin was added to one of them. Samples for microscopy were taken at each temperature shift, at rifampin addition, and at 35 and 70 min after the temperature shift back to 30°C. The proportions of cells with one *oriI* (*lacO*) focus, two foci touching each other, two foci segregated apart, three foci, four foci, and more than four foci are presented in the histogram. More than 500 cells were analyzed at each time point. (C) Time-lapse progression of *dnaC(Ts)* mutant cells with rifampin treatment. Cells were growing as previously described. After 2 h at 37°C, cells were shifted back to 30°C for 5 min to allow initiation of replication without changing much of the segregation pattern (compare column 3 to column 2 in panel B). Rifampin was then added to the culture for 10 min of incubation before cells were mounted on an agarose slide with medium and rifampin and visualized by time-lapse photography. *oriI* (*lacO*) is shown in green. An image was taken every 10 min.

the genetic distance between the unblocked and blocked loci. Blocking of any locus in the origin region (*oriI*, -2, -3, or -4) resulted in a very similar distance-related effect (summarized in Fig. 3A to D).

Finally, when replication was blocked at *R2* (*tetO*; midpoint of the right replichore), all of the *ori* markers segregated normally (Fig. 3F), demonstrating that blocking replication at later loci on one replication arm does not affect the segregation of the origin region. Interestingly, when replication was blocked at *R3* (*tetO*; ~ 700 kb from *dif*), the two replicated *L3* (*lacO*) foci, rather than segregating asymmetrically (57), were frequently placed on the outside of the two sister nucleoids, indicating that replication blockage near the end of replication can switch the sister nucleoid orientation as previously reported (38).

Our data (Fig. 3A to D) indicate that the mechanisms that govern the segregation of loci are the same for the left (L) and right (R) replichores, with no indication of a mechanism acting preferentially on either chromosome arm. Our analysis also demonstrates that early blockage (within the origin region) of one replication fork does not contribute to conversion of the normal <L-R-L-R> pattern of segregation to <L-R-R-L> or <R-L-L-R> (Fig. 3E and G), while late blockage of one replication fork switches nucleoid orientation, with sister loci derived from the blocked locus being located together in the nucleoid mid-region (38, 57).

Inhibition of RNA polymerase does not affect origin segregation. As both transcription and the insertion of newly transcribed-translated proteins into membrane (transertion) have been implicated as mechanisms contributing to bacterial chromosome segregation (12, 31, 45, 49, 61), we wished to test the consequence of inhibiting transcription (and thereby ongoing transertion) on segregation of *ori* loci. To do so, we synchronized cells for DNA synthesis using *dnaC(Ts)* mutation (40) and treated them with rifampin (300 μ g/ml) to block transcription. *dnaC(Ts)* mutant cells were grown exponentially at 30°C and then shifted to the nonpermissive temperature (37°C) at an A_{600} of ~ 0.1 to block replication initiation but allow completion of ongoing rounds of DNA synthesis. After 2 h, the cells were shifted back to 30°C for 5 min to allow initiation of DNA synthesis (47). The culture was subsequently split in two with rifampin added to one of them. The A_{600} of the rifampin-treated culture stopped increasing immediately after treatment, confirming that rifampin inhibited transcription effectively (Fig. 4A). Origin segregation was examined by snapshot fluorescence microscopy of cells with the *oriI* (*lacO*) marker (Fig. 4B). Following inhibition of replication initiation (2 h at 37°C), most of the cells (77%) had a single *oriI* focus, as expected. Cells with two foci were likely to be ones that were blocked for initiation but had not divided. After 5 min at the permissive temperature, during which replication initiation can occur, 73% of the cells retained a single focus. Although rep-

lication initiation occurs efficiently under these conditions, most of the newly replicated loci have not segregated (47, 59). By 70 min after replication initiation, the rifampin-treated and rifampin-free cultures showed essentially identical distributions of foci, with >80% of the cells containing two or more *oriI* foci. Nevertheless, 35 min after replication initiation, only 65% of the rifampin-treated cells had two or more *oriI* foci, compared to >80% of the cells in the nontreated control. Therefore, inhibition of transcription appeared to cause a slight delay of the replication-segregation process upon replication initiation.

In a parallel experiment in which rifampin was added 5 min before a shift back to the permissive temperature to allow replication initiation, >80% of the cells contained two or more foci after 70 min at the permissive temperature, while 56% of the cells contained two or more *oriI* foci at 35 min (data not shown). This result implies that inhibition of transcription does not prevent *ori* locus segregation but may delay replication initiation. Nevertheless, essentially all of the cells were able to initiate replication in a *dnaC*(Ts) strain shifted to the permissive temperature and to subsequently segregate newly replicated loci under conditions of transcription inhibition.

Time-lapse experiments confirmed the above observations (Fig. 4C). Following synchronization, cells were left at the permissive temperature for 5 min to allow replication initiation and then rifampin was added to the liquid culture for 10 min before the cells were mounted on the agarose slide containing growth medium and rifampin. During an 80-min time-lapse period, 20 of 36 rifampin-treated cells duplicated and separated their *oriI* sister foci more than one-third of a cell length apart, whereas the average cell length increased by only ~3% (compared to ~68% without rifampin treatment). An example is shown in Fig. 4C; the length of the rifampin-treated cell increased from 3.8 to 3.9 μm over 80 min, while the sister *oriI* loci segregated 1.4 μm apart between 20 and 30 min and were maximally 2.3 μm apart. This confirms that inhibition of transcription does not prevent segregation of newly replicated origins and that cell elongation is not necessary to allow *ori* segregation. Examination of the segregation of *R2* and loci within *ter* after rifampin treatment also showed that segregation of newly replicated copies of these loci was not blocked by inhibition of transcription (data not shown).

Inhibition of MreB dynamics does not affect origin segregation. Having shown that neither transcription nor cell growth along the long axis is necessary for *oriI* segregation, we examined the consequences of inhibiting the cytoskeletal protein MreB on *ori* locus segregation. In *C. crescentus*, A22, an inhibitor of the dynamic polymerization of the bacterial actin-like protein MreB, was reported to completely block the movement of newly replicated origins (20). Similarly, it was reported that after 1 h of A22 treatment, the percentage of *E. coli* cells with two *ori* foci decreased from 80% to 20%, suggesting that inhibiting MreB dynamics may also block origin segregation in *E. coli* (31). Furthermore, these same authors noted that cells expressing a mutant MreB protein failed to segregate their chromosomes normally (32). However, it has also been reported that A22 does not prevent chromosome segregation in *E. coli* (29). In an attempt to address this inconsistency, we used A22 to study the effect of MreB dynamics on origin segregation in our strain and under our experimental conditions. In all of our experiments, A22 (10 $\mu\text{g}/\text{ml}$) treatment

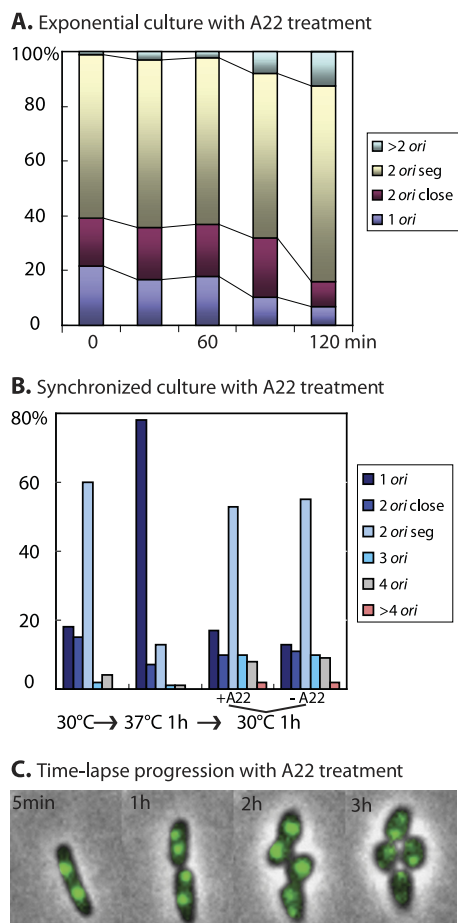


FIG. 5. A22 does not block origin segregation. (A) *ori* segregation in exponential culture before and after A22 treatment. Cells growing exponentially were harvested at different time points before and after A22 (10 $\mu\text{g}/\text{ml}$) treatment. The number of *oriI* (*lacO*) foci was analyzed and plotted. More than 500 cells were analyzed at each time point. (B) A22 does not block origin segregation after synchronization using *dnaC*(Ts) mutant cells. Cells were grown exponentially at 30°C and then shifted to 37°C for 1 h for synchronization. The culture was then split in two, one with and one without A22 treatment, and grown at 30°C for 1 h. Cells were harvested at each time point, and the *oriI* (*lacO*) foci in each cell were counted. The proportions of cells with different numbers of origins are shown. More than 500 cells were counted at each time point. (C) Time-lapse progression of cells treated with A22. Exponentially growing cells were treated with A22 for 1 min in liquid culture and subsequently mounted on an agarose slide containing medium and A22. Images were taken at 5 min, 1 h, 2 h, and 3 h after A22 treatment. *oriI* (*lacO*) was labeled green.

caused cells growing in minimal medium to slowly change their shape from rods to spheres through an egg-shaped intermediate. A strain with a single point mutation in MreB, making it resistant to A22 treatment, did not undergo the shape change (data not shown), showing that A22 did inhibit MreB function in our experiments.

To study the effect of A22 on *oriI* segregation, an exponential culture was split in two and one was treated with A22. Cells were harvested at various time points to score and compare the proportions of cells with one or more *oriI* foci. At all time points, the proportions remained similar with or without A22 treatment and an increase in cells with one *oriI* focus was not observed (Fig. 5A). Furthermore, when a *dnaC*(Ts) mutant

strain was used such that A22 could be added at the time of reinitiation of DNA synthesis, no difference was observed between the A22-treated cells and the nontreated control, again demonstrating no influence of A22 on *ori1* segregation (Fig. 5B). Finally, examination of A22-treated cells by time-lapse microscopy confirmed that cells continued to grow and segregate their *ori1* sister loci during A22 treatment (Fig. 5C).

Our data therefore support the view that inhibition of MreB dynamics does not prevent segregation of the origin region. Furthermore, we found that *L3*, *R3*, and loci in *ter* were also able to segregate normally after A22 treatment (data not shown), and therefore inhibition of MreB dynamics by A22 does not affect bulk chromosome segregation.

Dynamic locus behavior in the region of replication blocks. During initial time-lapse experiments of replication-blocked cells, we noted that with a replication-blocked *ori1* locus, the neighboring locus was sometimes seen to split into two closely spaced loci before reverting back to a single focus (Fig. 6A and B, 30-min block in liquid culture, followed by an additional 30 min on the slide before imaging, red arrows), thereby explaining some of the snapshot data (Fig. 3A to D). Furthermore, we occasionally observed a splitting of a blocked locus into two, before reversion to a single focus (Fig. 6B, green arrow). This behavior was not modified after rifampin treatment and was also observed in *RecA*⁻ cells, indicating that it is not a consequence of transcription/transertion or induced by DNA breakage-recombination (data not shown).

To gain insight into these observations, we constructed hybrid arrays in which 120 copies of *tetO* (4.1 kb) and 120 copies of *lacO* (4.3 kb) are immediately adjacent to each other. This tandem array hybrid was inserted at the *ori2* locus in both orientations, so that clockwise replication forks could encounter either the *lacO* or the *tetO* array first. Therefore, when replication was blocked at *tetO*, the behavior of *lacO* when either upstream or downstream of the block could be observed in time-lapse experiments.

When *lacO* was downstream of the block, only a single *lacO* focus, representing the unreplicated locus, was ever observed (Fig. 6C, 70-min block in liquid, followed by an additional 30 min on the slide before imaging; see movie S1 in the supplemental material). At most time points (93% in 25 time progressions, each of 14 time points), the *lacO* and *tetO* foci were superimposed.

When *lacO* was immediately upstream of the block, we observed frequent splitting and refusion of *lacO* foci (Fig. 6D, 70-min block in liquid, followed by an additional 30 min on the slide before imaging; see movie S2 in the supplemental material), indicating that a replication fork Y structure with two newly replicated copies of *lacO* adjacent to at least a partly unreplicated *tetO* locus allows spatial resolution of the sister *lacO* loci. Note that in these time-lapse progressions, as in those in Fig. 6C and D, the blocked locus exhibits an occasional splitting in two and refusion, indicating that the blocked locus has undergone at least partial replication, allowing some separation of the newly replicated *tetO* sisters. Analysis of 22 time-lapse progressions showed that the time during which the upstream *lacO* locus is split in two is about three times that of the blocked *tetO* locus.

The ability to spatially separate newly replicated sister *lacO* foci immediately adjacent to a blocked *tetO* locus was unex-

pected and shows that sister loci that are close and physically linked can be spatially separated. The length of an uncompact 4.3-kb *lacO* locus is 1.46 μm ; we do not know the conformation of such a locus *in vivo* and do not know how much of an array has to be bound by fluorescent repressors to give a focus. We would not expect sister copies of such a locus immediately behind a fork to become supercoiled because of the free DNA ends at the fork. Nevertheless, upon repressor binding, we observe a sharp focus indistinguishable from foci distant from replication forks. In Fig. 6D, the separated sister *lacO* foci are frequently $\geq 1 \mu\text{m}$ apart, with a smeary TetR-YFP trail between them. The 18- to 24-min time points in Fig. 6D are shown in Fig. 6E with the LacI-CFP (red) and TetR-YFP (green) channels placed side by side, along with a schematic that illustrates what we believe is the explanation for our observations. Assuming that the replication block is contained within the 4.1-kb *tetO* array, the centers of the upstream 4.3-kb sister *lacO* arrays can have a maximal spatial separation of 4.3 kb to $< 12.5 \text{ kb}$ (1.46 to 4.25 μm uncondensed), depending on whether the fork is blocked at the beginning of the *tetO* array or toward its end. The outer extremities of the newly replicated arrays could be up to 16.8 kb apart. About three kilobases of an uncondensed newly replicated locus bound by the repressor at its compacted outer extremity (Fig. 6E, schematic) would allow the type of spatial separation that we observed, with the uncondensed array sequence either lacking fluorescence or with a smear of fluorescence instead of a sharp focus.

Another explanation for the observed splitting of the *lacO* sisters when the downstream *tetO* locus is replication blocked is the arrival of a new round of replication at the blocked locus that generates a double-strand break at the blocked fork. This physical unlinking would allow separation of the *lacO* sisters as observed. Nevertheless, we do not favor this explanation since this behavior is observed in cells blocked for a period of only one generation (Fig. 6C and D) or less (Fig. 6A and B) before image capture commences. Because there are no overlapping rounds of replication under our growth conditions, most of the blocked forks would not be encountered by other replication forks from a new round of replication within the time course of the experiment. Furthermore, the same behavior is observed in *RecA*⁻ cells, in which we would not expect to see the refusion of the foci if the splitting were caused by double-strand breaks when new replication forks run into a blocked fork. We note that in these experiments, there is sufficient time for any pre-atenation present in the vicinity of the newly replicated sister loci to have been removed by TopoIV, which in turn may allow enough separation of the loci to explain the detectable splitting. These results provide new information on the spatial resolution of newly replicated loci using conventional epifluorescence microscopy and suggests dynamic behavior of newly replicated DNA in the region of a blocked fork.

DISCUSSION

The work presented here provides no support for the idea that transcription/transertion, MreB dynamics, or specific *cis*-acting DNA sequences play a key role in *E. coli* chromosome segregation. In cells with a single round of replication initiated and terminated in the same generation, segregation of the newly replicated sister loci of the *ori* region on different repli-

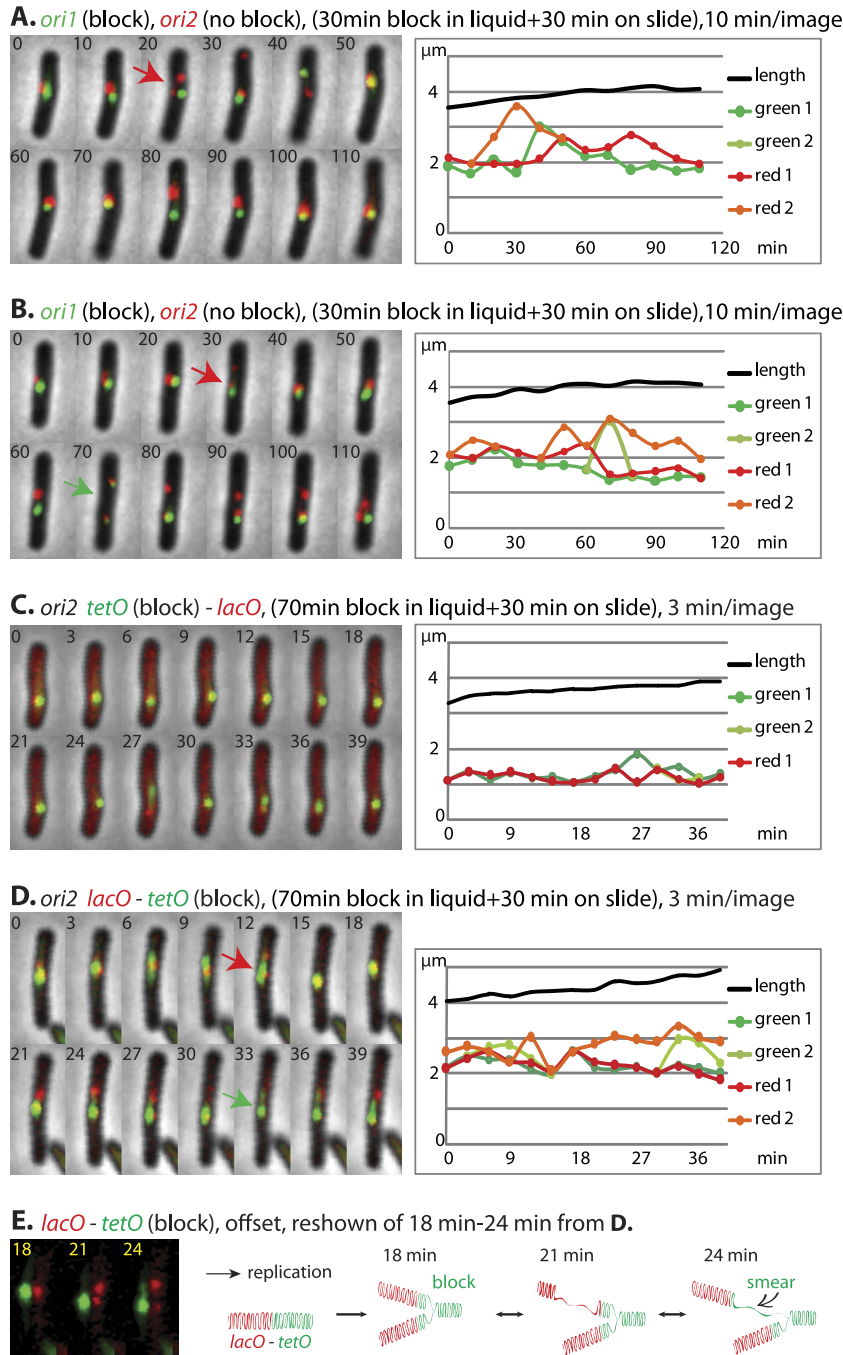


FIG. 6. Dynamics of replication block by TetR binding to *tetO* in time-lapse progressions (left) and their plots (right). (A and B) Dynamics of *ori1* and *ori2* during replication block at *ori1* (*tetO*). To induce a block, cells were grown in liquid culture for 30 min without AT, followed by another 30 min without AT on the slide. An image was taken every 10 min. Red and green arrows show the splitting and refusion of the nonblocked locus and the blocked locus, respectively. (C and D) Dynamic behavior of tandem *tetO-lacO* or *lacO-tetO* arrays at *ori2*. In panel C, the *lacO* array (labeled red) is downstream of the *tetO* (green) block. In panel D, the *lacO* array (labeled red) is upstream of the *tetO* (green) block. Red and green arrows show the splitting and refusion of the nonblocked locus and the blocked locus, respectively. The block was induced for 70 min in liquid culture, followed by an additional 30 min on the slide before image capture. Images were taken every 3 min. (E) Eighteen- to 24-min time points from panel D with the TetR-YFP (green) and LacI-CFP (red) channels placed side by side for clarity. The schematic on the right illustrates the explanation. Condensed *lacO* and *tetO* arrays are shown as red and green helices. Replication block occurs within the *tetO* array, which allows replication of the upstream *lacO* array. At 18 min, both the *lacO* and *tetO* arrays were condensed, giving one red focus and one green focus overlapping due to the limitation of spatial resolution. At 21 min, 2 to 3 kb of DNA in one of the replicated *lacO* arrays was relaxed, or stretched by the upstream DNA regions (not illustrated), so that the beginning of that *lacO* array was separated far enough to give a separate focus. At 24 min, some of the replicated *tetO* array was condensed with the upstream *lacO* array, leaving a smear of TetR-YFP (green) fluorescence labeling the uncondensed region. Note that YFP is significantly brighter than CFP owing to the properties of the different fluorophores, which is why the smear of the CFP (labeled red) channel is not visible or is less clear.

chores is sequential, independent, and apparently symmetrical. Blocking of replication in one replicore does not prevent segregation of loci on the other.

It seems plausible that spontaneous chromosome segregation by entropic disentanglement of the chromosomal polymer (1, 27, 28) may provide the essence of the segregation mechanism. Therefore, the key to efficient and faithful segregation is likely to reside in chromosome organization itself and the processes that drive this organization, as well as independent replication by spatially separated replisomes tracking along the DNA and the subsequent decatenation by TopoIV. Consistent with this view, aberrant chromosome organization as a consequence of absence of functional SMC complexes (MukBEF) leads to an altered pattern of replication-segregation and to failures in chromosome segregation (8, 10, 44). It seems to us that the independent tracking of sister replisomes along DNA, outward from *oriC* (47), may facilitate the segregation of newly replicated sister chromosomes into separate cell halves, thereby allowing the entropic mechanism to mediate the segregation process efficiently.

ACKNOWLEDGMENTS

We thank R. Reyes-Lamothe for the kind gift of the *ypet-dnaN* strain, K. Gerdes for the A22-resistant *mreB* mutant strain, and H. Niki for the *migS* deletion strain.

This research was supported by the Wellcome Trust.

REFERENCES

- Arnold, A., and S. Jun. 2007. Time scale of entropic segregation of flexible polymers in confinement: implications for chromosomal segregation in filamentous bacteria. *Phys. Rev. E Stat. Nonlin. Soft Matter Phys.* **76**(Pt. 1):031901.
- Bates, D., and N. Kleckner. 2005. Chromosome and replisome dynamics in *E. coli*: loss of sister cohesion triggers global chromosome movement and mediates chromosome segregation. *Cell* **121**:899–911.
- Bean, G. J., S. T. Flickinger, W. M. Westler, M. E. McCully, D. Sept, D. B. Weibel, and K. J. Amann. 2009. A22 disrupts the bacterial actin cytoskeleton by directly binding and inducing a low-affinity state in MreB. *Biochemistry* **48**:4852–4857.
- Becker, E., N. C. Herrera, F. Q. Gunderson, A. I. Derman, A. L. Dance, J. Sims, R. A. Larsen, and J. Pogliano. 2006. DNA segregation by the bacterial actin Alfa during *Bacillus subtilis* growth and development. *EMBO J.* **25**:5919–5931.
- Ben-Yehuda, S., D. Z. Rudner, and R. Losick. 2003. RacA, a bacterial protein that anchors chromosomes to the cell poles. *Science* **299**:532–536.
- Bowman, G. R., L. R. Comolli, J. Zhu, M. Eckart, M. Koenig, K. H. Downing, W. E. Moerner, T. Earnest, and L. Shapiro. 2008. A polymeric protein anchors the chromosomal origin/ParB complex at a bacterial cell pole. *Cell* **134**:945–955.
- Breier, A. M., and A. D. Grossman. 2007. Whole-genome analysis of the chromosome partitioning and sporulation protein Spo0J (ParB) reveals spreading and origin-distal sites on the *Bacillus subtilis* chromosome. *Mol. Microbiol.* **64**:703–718.
- Britton, R. A., D. C. Lin, and A. D. Grossman. 1998. Characterization of a prokaryotic SMC protein involved in chromosome partitioning. *Genes Dev.* **12**:1254–1259.
- Daniel, R. A., and J. Errington. 2003. Control of cell morphogenesis in bacteria: two distinct ways to make a rod-shaped cell. *Cell* **113**:767–776.
- Danilova, O., R. Reyes-Lamothe, M. Pinskaya, D. Sherratt, and C. Possoz. 2007. MukB colocalizes with the *oriC* region and is required for organization of the two *Escherichia coli* chromosome arms into separate cell halves. *Mol. Microbiol.* **65**:1485–1492.
- Datsenko, K. A., and B. L. Wanner. 2000. One-step inactivation of chromosomal genes in *Escherichia coli* K-12 using PCR products. *Proc. Natl. Acad. Sci. U. S. A.* **97**:6640–6645.
- Dworkin, J., and R. Losick. 2002. Does RNA polymerase help drive chromosome segregation in bacteria? *Proc. Natl. Acad. Sci. U. S. A.* **99**:14089–14094.
- Ebersbach, G., A. Briegel, G. J. Jensen, and C. Jacobs-Wagner. 2008. A self-associating protein critical for chromosome attachment, division, and polar organization in *Caulobacter*. *Cell* **134**:956–968.
- Ebersbach, G., and K. Gerdes. 2005. Plasmid segregation mechanisms. *Annu. Rev. Genet.* **39**:453–479.
- Espeli, O., R. Mercier, and F. Boccard. 2008. DNA dynamics vary according to macromolecule topography in the *E. coli* chromosome. *Mol. Microbiol.* **68**:1418–1427.
- Fekete, R. A., and D. K. Chatteraj. 2005. A *cis*-acting sequence involved in chromosome segregation in *Escherichia coli*. *Mol. Microbiol.* **55**:175–183.
- Figge, R. M., A. V. Divakaruni, and J. W. Gober. 2004. MreB, the cell shape-determining bacterial actin homologue, co-ordinates cell wall morphogenesis in *Caulobacter crescentus*. *Mol. Microbiol.* **51**:1321–1332.
- Fogel, M. A., and M. K. Waldor. 2006. A dynamic, mitotic-like mechanism for bacterial chromosome segregation. *Genes Dev.* **20**:3269–3282.
- Garner, E. C., C. S. Campbell, D. B. Weibel, and R. D. Mullins. 2007. Reconstitution of DNA segregation driven by assembly of a prokaryotic actin homolog. *Science* **315**:1270–1274.
- Gitai, Z., N. A. Dye, A. Reisenauer, M. Wachi, and L. Shapiro. 2005. MreB actin-mediated segregation of a specific region of a bacterial chromosome. *Cell* **120**:329–341.
- Gruber, S., and J. Errington. 2009. Recruitment of condensin to replication origin regions by ParB/Spo0J promotes chromosome segregation in *B. subtilis*. *Cell* **137**:685–696.
- Heidelberg, J. F., J. A. Eisen, W. C. Nelson, R. A. Clayton, M. L. Gwinn, R. J. Dodson, D. H. Haft, E. K. Hickey, J. D. Peterson, L. Umayam, S. R. Gill, K. E. Nelson, T. D. Read, H. Tettelin, D. Richardson, M. D. Ermolaeva, J. Vamathevan, S. Bass, H. Qin, I. Dragoi, P. Sellers, L. McDonald, T. Utterback, R. D. Fleischmann, W. C. Nierman, O. White, S. L. Salzberg, H. O. Smith, R. R. Colwell, J. J. Mekalanos, J. C. Venter, and C. M. Fraser. 2000. DNA sequence of both chromosomes of the cholera pathogen *Vibrio cholerae*. *Nature* **406**:477–483.
- Iretton, K., N. W. Gunther, and A. D. Grossman. 1994. *spo0J* is required for normal chromosome segregation as well as the initiation of sporulation in *Bacillus subtilis*. *J. Bacteriol.* **176**:5320–5329.
- Iwai, N., K. Nagai, and M. Wachi. 2002. Novel S-benzylisothiourea compound that induces spherical cells in *Escherichia coli* probably by acting on a rod-shape-determining protein(s) other than penicillin-binding protein 2. *Biosci. Biotechnol. Biochem.* **66**:2658–2662.
- Jacob, F., S. Brenner, and F. Cuzin. 1963. On the regulation of DNA replication in bacteria. *Cold Spring Harb. Symp. Quant. Biol.* **28**:329–348.
- Jones, L. J., R. Carballido-Lopez, and J. Errington. 2001. Control of cell shape in bacteria: helical, actin-like filaments in *Bacillus subtilis*. *Cell* **104**:913–922.
- Jun, S., and B. Mulder. 2006. Entropy-driven spatial organization of highly confined polymers: lessons for the bacterial chromosome. *Proc. Natl. Acad. Sci. U. S. A.* **103**:12388–12393.
- Jun, S., and A. Wright. 2010. Entropy as the driver of chromosome segregation. *Nat. Rev. Microbiol.* **8**:600–607.
- Karczmarek, A., R. Martinez-Arteaga, S. Alexeeva, F. G. Hansen, M. Vicente, N. Nanninga, and T. den Blaauwen. 2007. DNA and origin region segregation are not affected by the transition from rod to sphere after inhibition of *Escherichia coli* MreB by A22. *Mol. Microbiol.* **65**:51–63.
- Kim, H. J., M. J. Calcult, F. J. Schmidt, and K. F. Chater. 2000. Partitioning of the linear chromosome during sporulation of *Streptomyces coelicolor* A3(2) involves an *oriC*-linked *parAB* locus. *J. Bacteriol.* **182**:1313–1320.
- Kruse, T., B. Blagoev, A. Lobner-Olesen, M. Wachi, K. Sasaki, N. Iwai, M. Mann, and K. Gerdes. 2006. Actin homolog MreB and RNA polymerase interact and are both required for chromosome segregation in *Escherichia coli*. *Genes Dev.* **20**:113–124.
- Kruse, T., J. Moller-Jensen, A. Lobner-Olesen, and K. Gerdes. 2003. Dysfunctional MreB inhibits chromosome segregation in *Escherichia coli*. *EMBO J.* **22**:5283–5292.
- Lau, I. F., S. R. Filipe, B. Soballe, O. A. Okstad, F. X. Barre, and D. J. Sherratt. 2003. Spatial and temporal organization of replicating *Escherichia coli* chromosomes. *Mol. Microbiol.* **49**:731–743.
- Lemon, K. P., and A. D. Grossman. 2001. The extrusion-capture model for chromosome partitioning in bacteria. *Genes Dev.* **15**:2031–2041.
- Lewis, R. A., C. R. Bignell, W. Zeng, A. C. Jones, and C. M. Thomas. 2002. Chromosome loss from *par* mutants of *Pseudomonas putida* depends on growth medium and phase of growth. *Microbiology* **148**:537–548.
- Li, Y., K. Sergueev, and S. Austin. 2002. The segregation of the *Escherichia coli* origin and terminus of replication. *Mol. Microbiol.* **46**:985–996.
- Lin, D. C., and A. D. Grossman. 1998. Identification and characterization of a bacterial chromosome partitioning site. *Cell* **92**:675–685.
- Liu, X., X. Wang, R. Reyes-Lamothe, and D. Sherratt. 2010. Replication-directed sister chromosome alignment in *Escherichia coli*. *Mol. Microbiol.* **75**:1090–1097.
- Livny, J., Y. Yamaichi, and M. K. Waldor. 2007. Distribution of centromere-like *parS* sites in bacteria: insights from comparative genomics. *J. Bacteriol.* **189**:8693–8703.
- Maisnier-Patin, S., K. Nordström, and S. Dasgupta. 2001. Replication arrests during a single round of replication of the *Escherichia coli* chromosome in the absence of DnaC activity. *Mol. Microbiol.* **42**:1371–1382.
- Mohl, D. A., and J. W. Gober. 1997. Cell cycle-dependent polar localization of chromosome partitioning proteins in *Caulobacter crescentus*. *Cell* **88**:675–684.

42. Murray, H., H. Ferreira, and J. Errington. 2006. The bacterial chromosome segregation protein Spo0J spreads along DNA from *parS* nucleosome sites. *Mol. Microbiol.* **61**:1352–1361.
43. Nielsen, H. J., Y. Li, B. Youngren, F. G. Hansen, and S. Austin. 2006. Progressive segregation of the *Escherichia coli* chromosome. *Mol. Microbiol.* **61**:383–393.
44. Niki, H., A. Jaffe, R. Imamura, T. Ogura, and S. Hiraga. 1991. The new gene *mu kb* codes for a 177 kd protein with coiled-coil domains involved in chromosome partitioning of *E. coli*. *EMBO J.* **10**:183–193.
45. Norris, V. 1995. Hypothesis: transcriptional sensing and membrane-domain formation initiate chromosome replication in *Escherichia coli*. *Mol. Microbiol.* **15**:985–987.
46. Possoz, C., S. R. Filipe, I. Grainge, and D. J. Sherratt. 2006. Tracking of controlled *Escherichia coli* replication fork stalling and restart at repressor-bound DNA *in vivo*. *EMBO J.* **25**:2596–2604.
47. Reyes-Lamothe, R., C. Possoz, O. Danilova, and D. J. Sherratt. 2008. Independent positioning and action of *Escherichia coli* replisomes in live cells. *Cell* **133**:90–102.
48. Ringgaard, S., J. van Zon, M. Howard, and K. Gerdes. 2009. Movement and equipositioning of plasmids by ParA filament disassembly. *Proc. Natl. Acad. Sci. U. S. A.* **106**:19369–19374.
49. Rocha, E. P., J. Fralick, G. Vedyappan, A. Danchin, and V. Norris. 2003. A strand-specific model for chromosome segregation in bacteria. *Mol. Microbiol.* **49**:895–903.
50. Soppa, J. 2001. Prokaryotic structural maintenance of chromosomes (SMC) proteins: distribution, phylogeny, and comparison with MukBs and additional prokaryotic and eukaryotic coiled-coil proteins. *Gene* **278**:253–264.
51. Soufo, H. J., and P. L. Graumann. 2003. Actin-like proteins MreB and Mbl from *Bacillus subtilis* are required for bipolar positioning of replication origins. *Curr. Biol.* **13**:1916–1920.
52. Sullivan, N. L., K. A. Marquis, and D. Z. Rudner. 2009. Recruitment of SMC by ParB-*parS* organizes the origin region and promotes efficient chromosome segregation. *Cell* **137**:697–707.
53. Thanbichler, M., and L. Shapiro. 2006. MipZ, a spatial regulator coordinating chromosome segregation with cell division in *Caulobacter*. *Cell* **126**:147–162.
54. Toro, E., S. H. Hong, H. H. McAdams, and L. Shapiro. 2008. *Caulobacter* requires a dedicated mechanism to initiate chromosome segregation. *Proc. Natl. Acad. Sci. U. S. A.* **105**:15435–15440.
55. Viollier, P. H., M. Thanbichler, P. T. McGrath, L. West, M. Meewan, H. H. McAdams, and L. Shapiro. 2004. Rapid and sequential movement of individual chromosomal loci to specific subcellular locations during bacterial DNA replication. *Proc. Natl. Acad. Sci. U. S. A.* **101**:9257–9262.
56. Waldminghaus, T., and K. Skarstad. 2009. The *Escherichia coli* SeqA protein. *Plasmid* **61**:141–150.
57. Wang, X., X. Liu, C. Possoz, and D. J. Sherratt. 2006. The two *Escherichia coli* chromosome arms locate to separate cell halves. *Genes Dev.* **20**:1727–1731.
58. Wang, X., C. Possoz, and D. J. Sherratt. 2005. Dancing around the divisome: asymmetric chromosome segregation in *Escherichia coli*. *Genes Dev.* **19**:2367–2377.
59. Wang, X., R. Reyes-Lamothe, and D. J. Sherratt. 2008. Modulation of *Escherichia coli* sister chromosome cohesion by topoisomerase IV. *Genes Dev.* **22**:2426–2433.
60. Webb, C. D., P. L. Graumann, J. A. Kahana, A. A. Teleman, P. A. Silver, and R. Losick. 1998. Use of time-lapse microscopy to visualize rapid movement of the replication origin region of the chromosome during the cell cycle in *Bacillus subtilis*. *Mol. Microbiol.* **28**:883–892.
61. Woldringh, C. L. 2002. The role of co-transcriptional translation and protein translocation (transertion) in bacterial chromosome segregation. *Mol. Microbiol.* **45**:17–29.
62. Wu, L. J., and J. Errington. 2003. RacA and the Soj-Spo0J system combine to effect polar chromosome segregation in sporulating *Bacillus subtilis*. *Mol. Microbiol.* **49**:1463–1475.
63. Yamaichi, Y., M. A. Fogel, and M. K. Waldor. 2007. *par* genes and the pathology of chromosome loss in *Vibrio cholerae*. *Proc. Natl. Acad. Sci. U. S. A.* **104**:630–635.
64. Yamaichi, Y., and H. Niki. 2004. *migS*, a *cis*-acting site that affects bipolar positioning of *oriC* on the *Escherichia coli* chromosome. *EMBO J.* **23**:221–233.